A Statistical Clutter Suppression Method Based on Given Target-Existence Probabilities for High Resolution UWB Radars

Satoshi Takahashi
Faculty of Information Sciences, Hiroshima City University
3–4–1 Ozuka-Higashi, Asa-Minami, Hiroshima 731–3194, Japan
e-mail: s.takahashi@m.ieice.org

Chang-Jun Ahn
Faculty of Information Sciences, Hiroshima City University
3–4–1 Ozuka-Higashi, Asa-Minami, Hiroshima 731–3194, Japan
e-mail: junny@m.ieice.org

***Abstract*— High-resolution radars (HRR) using ultra wideband (UWB) signals is a promising system for various detection and ranging applications. The radar resolution increases as a decrease of the pulse width, then radar echoes including background unwanted ones become spiky. Various modifications of constant false alarm rate (CFAR) and matched filters have been proposed to reduce false alarm induced by unwanted radar echos (clutter), but the target shape information diminishes due to exploitations based on range-bin processing. In this paper, a method of suppressing clutter with the reception power conversion is proposed. Novel categories of reflection objects with their existence probabilities are introduced and the characteristic function method is used for efficiently obtaining the power conversion table on a computer.**

***Keywords*— UWB radar, HRR (high-resolution radar), radar clutter, power conversion, target-existence probability**

I. Introduction

High resolution radars (HRR) using ultra wideband (UWB) are promising for various detection and ranging applications such as automotive and medical use.

Radar reception signals often contain unwanted echoes, and such echoes clutter the wanted target signal. The unwanted echoes make it difficult to determine the target and are called "radar clutter." Clutter is sometimes larger than the target signal and causes higher false alarms. Because what echoes are clutter is application-dependent, the clutter suppression methods exploit the characteristics of the target and clutter echoes. Moving target indication (MTI) for weather and airport surveillance radars culls non-fluctuating signals during pulse-to-pulse intervals to diminish echoes from mountains. Constant false alarm rate (CFAR) circuits for maritime radars use an average amplitude within several range bins to alleviate sea clutter on the assumption that target signals do not vary and that clutter amplitudes are Rayleigh distributed [1]. CFAR adjusts the threshold adaptively by using the average range-bin samples.

The radar resolution increases as a decrease of the pulse width, then radar echoes tend to be spiky in time or distance range domain. For an example of sea clutter, there are many echoes from sea surface facets within the radar illumination area and the resulting signal obeys Rayleigh distribution because of the central limit theorem. For HRR, however, a few facets contribute the resulting sea clutter and their mutual echo interferences characterize spiky clutter [2]. The amplitude fluctuation has assumed to be as Weibull distribution, log-normal distribution, and K-distribution, and various modifications of CFAR circuits [3] as well as use of matched filters [4], [5], [6] have been proposed. In these CFAR modifications, both the average and variance of range bins are used to fit these two-parameter distributions and to obtain the optimum threshold for clutters. UWB radars, however, the target shape information diminishes due to their exploitations based on range-bin basis signal processing.

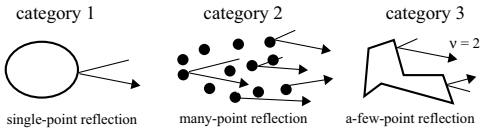

Fig. 1. Categories of reflection objects.

In this paper, a method of suppressing clutter by using the reception power conversion is proposed. Novel categories of reflection objects with their existence probabilities are introduced to represent UWB radar echoes and it enables us to distinguish fluctuating target that obeys a specific distribution from clutter objects. Once the distribution parameters of target signal and clutter are determined, for example by measurements, the power conversion table that weakens the spikes can be derived immediately. The characteristic function method in the Fourier series form is used for efficiently obtaining the power conversion table on a computer. First, object categories for UWB radars are introduced and their mathematical expression is shown. Then a method of suppressing clutter is presented. Finally, an example of the power correction curve and the numerical results are shown.

II. Categories of Reflection Objects

Radar signals fluctuate due to slight environmental changes such as the target movements, and the fluctuation is characterized by the ratio of the radar illumination area to the reflecting facets area. The conventional threshold detection and CFAR methods assume that sufficiently large number of echoes reflected from a clutter object lead to Rayleigh distribution in the amplitude expression, or exponential distribution in the power expression.

For improving signal-to-clutter ratios, the pulse integration techniques have often been employed. It averages over pulse-to-pulse reception signals at the same range bins. Fluctuation level interval of clutter diminishes as the number of integration pulses increases, and it results in a higher signal-to-clutter ratio. Rayleigh-distributed clutter becomes χ(chi)-squared distribution by the pulse integration [1].

A UWB signal is virtually carrier-less. Therefore, the signal is processed incoherently and we use the signal expression of reception power instead of amplitude. Then the clutter obeys the exponential distribution for the single-pulse detection and the gamma distribution with m degrees for pulse integration processes of m times.

Conventional radar detection uses two categories of the target and others. In contrast, we categorize reflections in terms of the statistical number of radiowaves within the radar illumination area. Figure 1 illustrates radar echoes categories used here. A signal reflected of an object larger than the radar illumination area is steady and does not vary during pulse-to-pulse intervals. We define

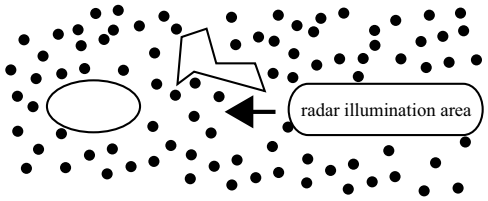

Fig. 2. Actual environment that consists of categories 1–3 reflection objects.

such reflection as category 1 reflection. The probability density function (pdf) of the reception power $p_1(x)$ can be expressed as

$$p_1(x) = \delta(x - x_1), \tag{1}$$

where x_1 is the reflection power of the category 1 object, and $\delta(\cdot)$ is the delta function defined by

$$\delta(x) = \begin{cases} 1 & \text{for } x = 0 \\ 0 & \text{otherwise.} \end{cases}$$

On the other hand, there are multiple reflection points within the radar illumination area and the resultant amplitude follows Rayleigh distribution. We define the situation as category 2. In our power expression, it obeys negative exponential distribution due to the variable conversion [2]. The pdf $p_2(x)$ is

$$p_2(x) = \frac{1}{x_2} \exp\left(-\frac{x}{x_2}\right) u(x), \tag{2}$$

where x_2 is the mean reflection power of the category 2 object and $u(\cdot)$ is the unit function defined by

$$u(x) = \begin{cases} 1 & \text{for } 0 \geq 0 \\ 0 & \text{otherwise.} \end{cases}$$

A situation where there are few reflections contribute to the reception signal is defined as category 3. According to elaborate study of laser speckle patterns of Jakeman and Tough, the power variation follows gamma distribution [7]. The pdf $p_3(x)$ is

$$p_3(x) = \gamma x^{\nu-1} \exp\left(-\frac{x}{x_3}\right) u(x), \tag{3}$$

where x_3 is the mean reflection power of the category 3 object and γ is the normalization coefficient given by

$$\gamma = \frac{1}{x_3^{\nu}\,\Gamma(\nu+1)},$$

where $\Gamma(\cdot)$ is the gamma function. The gamma distribution is source of the birth-death-migration random process of varied scatterer numbers that expresses the radar illumination-area movement. The shape parameter ν appeared in Eq.(3) can be interpreted as the number of reflection waves. The shape parameter must be positive and is possibly less than 1 where the reflection occurs rarely.

In an actual environment, there are category 1, 2, and 3 objects with certain probabilities. For example in a car-borne UWB HRR radar, category 1 objects are cars with an existence probability of 5% of the whole measurement space, category 2 objects are receiver noise and human body surface with an existence probability of 80%, and category 3 objects may be road surface, bicycles, guard rails with an existence probability of 15%. Radar illumination area associated with the transmitted pulse width moves as time elapses as shown in Fig. 2, and some radiowaves reflected or backscattered to the radar antenna. Though the percentages of categories 1–3 objects within the area, the statistical reception power can be expressed as the mean powers and the existence probabilities of them. The reception power obeys the compound distribution of them.

III. Mathematical Expression of Radar Reception Power

The characteristic function method and its Fourier expansion form is used for expressing the reception power distribution here. The characteristic function (chf) $\Phi(\omega)$ is obtained using the modified Fourier transform of the original pdf $p(x)$,

$$\Phi(\omega) = \int_{-\infty}^{\infty} p(x)\, e^{j\omega t}\, dt, \tag{4}$$

and the pdf can be derived from the chf with the modified inverse Fourier transform [8],

$$p(x) = \frac{1}{2\pi} \int_{-\infty}^{\infty} \Phi(\omega)\, e^{-j\omega t}\, d\omega, \tag{5}$$

where ω is an auxiliary variable. With the scaling technique, the chf representing the compound distribution resulted from category 1–3 reflections $\Phi(\omega)$ can be written by the weighted product of their chfs,

$$\Phi(\omega) = \Phi_1(c_1\omega) \cdot \Phi_2(c_2\omega) \cdot \Phi_3(c_3\omega), \tag{6}$$

where c_1, c_2 and c_3 are the existence probabilities of the category 1–3, and $c_1 + c_2 + c_3 = 1$. Applying Eq.(4) to Eqs.(1), (2), and (3), $\Phi_1(\omega)$, $\Phi_2(\omega)$, and $\Phi_3(\omega)$ are:

$$\begin{aligned} \Phi_1(\omega) &= \exp(j\omega x_1), \\ \Phi_2(\omega) &= \frac{1}{(1 - j\omega x_2)}, \text{ and} \\ \Phi_3(\omega) &= \frac{1}{(1 - j\omega x_3)^{\nu}}. \end{aligned} \tag{7}$$

Then the pdf can be obtained from Eq.(7) using Eq.(5). The reception power chf after m times pulse integration can easily derived from a slight modification of Eq.(6):

$$\Phi(\omega) = \Phi_1\left(\frac{c_1\,\omega}{m}\right)^m \cdot \Phi_2\left(\frac{c_2\,\omega}{m}\right)^m \cdot \Phi_3\left(\frac{c_3\,\omega}{m}\right)^m. \tag{8}$$

Though Eq.(5) involves the infinite-range integral, the distribution can efficiently be obtained because the reception power is not infinity. The power limited Fourier expansion is proposed [9]. When the maximum power of x is R, Eq.(4) is rewrited to

$$\Phi(\omega) = \int_{-R}^{R} p(x)\, \exp\left(j\omega t\right)\, dt, \tag{9}$$

On the other hand, a pdf $p(x)$ can be expressed by

$$p(x) = \sum_{n=-\infty}^{\infty} f_n \exp\left(j\frac{n\pi}{R}x\right), \tag{10}$$

where f_n is the Fourier series,

$$f_n = \frac{1}{2R} \int_{-R}^{R} p(x) \exp\left(-j\frac{n\pi}{R}x\right)\, dx. \tag{11}$$

Comparing Eqs.(9) and (11), we obtain

$$f_n = \frac{1}{2R}\Phi(-\frac{n\pi}{R}). \tag{12}$$

Substituting Eq.(12) into Eq.(10), we obtain generic form of the pdf provided in [9]:

$$\begin{aligned} p(x) &= \frac{1}{2R} \sum_{n=-\infty}^{\infty} \Phi\left(\frac{n\pi}{R}\right) \exp\left(-j\frac{n\pi}{R}x\right) \\ &= \frac{1}{2R}\left[1 + 2\sum_{n=1}^{\infty} \text{Re}\,\left\{\Phi\left(\frac{n\pi}{R}\right)\right\} \cos\frac{n\pi}{R}x \right. \\ &\quad \left. + 2\sum_{n=1}^{\infty} \text{Im}\,\left\{\Phi\left(\frac{n\pi}{R}\right)\right\} \sin\frac{n\pi}{R}x\right] \end{aligned} \tag{13}$$

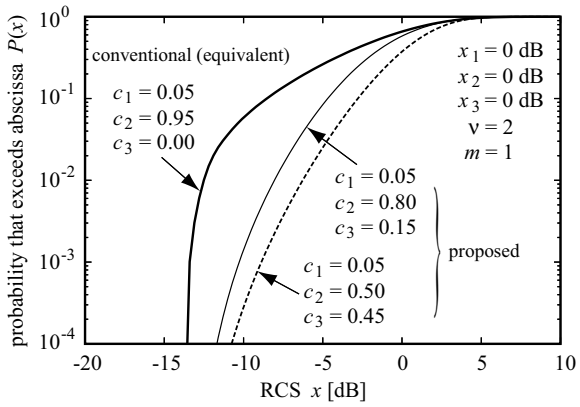

Fig. 3. Reception power distribution for various target-existence probabilities.

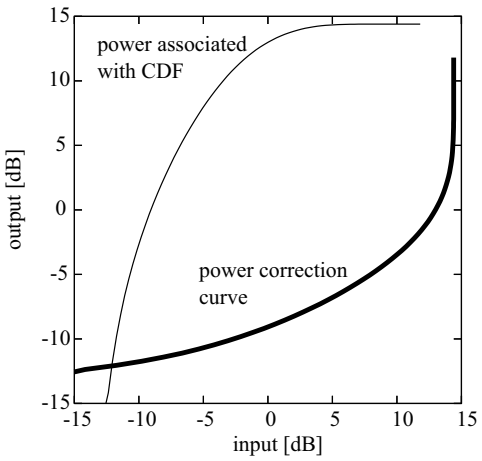

Fig. 4. An example of the power correction curve.

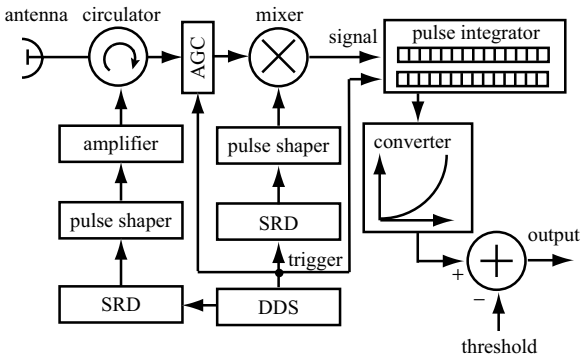

Fig. 5. Block diagram for the proposed clutter suppression.

By termwise integration of the pdf, we obtain the cumulative distribution function (cdf) of the reception power:

$$\begin{aligned} P(x) &= \int_0^x p(x)dx \\ &= \frac{x}{2R} + \sum_{n=1}^{\infty} \frac{1}{n\pi} \left[\mathrm{Re} \left\{ \Phi\left(\frac{n\pi}{R}\right) \right\} \sin \frac{n\pi}{R} x \right. \\ &- \left. \mathrm{Im} \left\{ \Phi\left(\frac{n\pi}{R}\right) \right\} \left(\cos \frac{n\pi}{R} x - 1 \right) \right] \end{aligned} \tag{14}$$

We have plotted cdf of Eq.(14) in Fig. 3 for various target-existence probabilities. A single pulse detection ($m = 1$) is assumed in the plot. The series in Eq.(14) has the infinite number of terms, but it is enough to use 1,000 terms at most. The maximum power is set to $R = x_1 + 10\,(x_2 + x_3)$. The abscissa is the radar cross section (RCS) that shows a reception power as an area ratio whose base is uniformly scattered power for all directions, and the dimension is the power ratio [1]. The ordinate shows probability that exceed the abscissa. Conventional methods do not assume the category 2 objects. Therefore, we estimate the conventional suppression method where c_2 is set to zero. On the other hand, the ratio of the existence probability of categories 2 and 3 varies in the proposed estimation, and the sum of the probabilities is equal to the category 2 of the conventional estimation. The shape parameter for the category 3 target here is 2. A size of illumination area of UWB HRR is several hundreds millimeter. Therefore, it is natural to choose $\nu = 2$ where we assume a car-borne radar and the category 3 targets are bicycles and guard rails. The mean reception powers for all categories are set to the same in the estimation so that we can know the dependence of the existence probabilities. The figure shows that the target-existence probabilities can influence the resultant reception signal characteristics. The conventional estimation curve was steep; it means the most of reception signal samples have a certain power and a few samples have a higher power. Comparing it with the conventional curve, proposed estimation curves lay. In the case, false alarm is high. The conventional estimation is optimistic.

IV. Statistical Clutter Suppression and Its Numerical Examples

For a higher false alarm cases due to spiky reflection objects, we propose the use of a power conversion table that smoothes the spikes in reception signal. If we correspond the cdf values to powers (or intensity in CRT display) produces a conversion table. Wide variation of reception power has converted to a narrower variation. A example of the conversion table is shown in Fig. 4. In the plot, the category 1 target with an existence probability of $c_1 = 0.05$, the background scatterer with an existence probability of $c_2 = 0.80$, the spiky scatterer with an existence probability of $c_3 = 0.15$, and a shape parameter of $\nu = 2$ are assumed. The thin curve in Fig. 4 is plotted that we correspond the output power as "$6\,\{\log_{10} P(x) + 2.4\}$ [dB]," for an example, for an input power of x [dB]. The conversion table shown in thick curve is obtained interchanging the input and output of the thin curve. A block diagram for the proposed clutter suppression is shown in Fig. 5. It consists of step recovery diodes (SRD), pulse shapers, power amplifier, circulator, mixer, direct digital synthesizers (DDS), pulse integrator, automatic gain control (AGC) circuit, and the power converter.

If we assume the target of category 1, the target can be extracted easily with the cdf of reception power, since the power conversion of the inverse cdf conserve the spiky reception signal constant and the reception power contribution of category 1 signal is steady.

The dependence of the number of pulses integrated on the cdf is shown in Fig. 6. We assumed the parameters above except for the mean power of the category 1 target. For obtaining the effect of the pulse integration, we have applied the exception. The probability curve becomes steeper as the integration number increases, and it showed that the spike was smoothed by the integration.

The dependence of the shape parameter on the cdf is also shown in Fig. 7. The same exception as in the pulse integration was also applied to this evaluation. The lower the shape parameter was, the steeper the curve was. Therefore, it is important to know accurate shape parameter especially the case that the parameter is low, say less than 1.

V. Conclusion

Novel categories of reflection objects were introduced to accurately obtain the reception power distribution of UWB radar. The

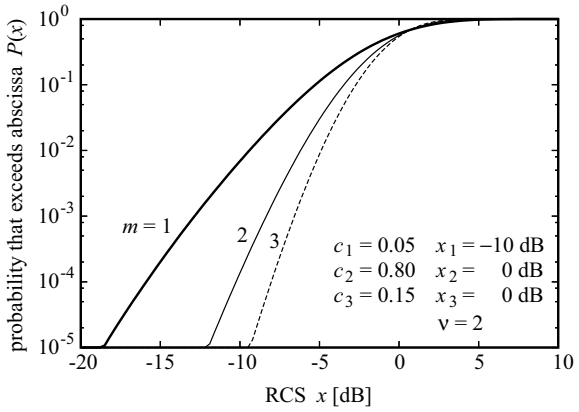

Fig. 6. Dependence of the probability on the number of pulses integrated.

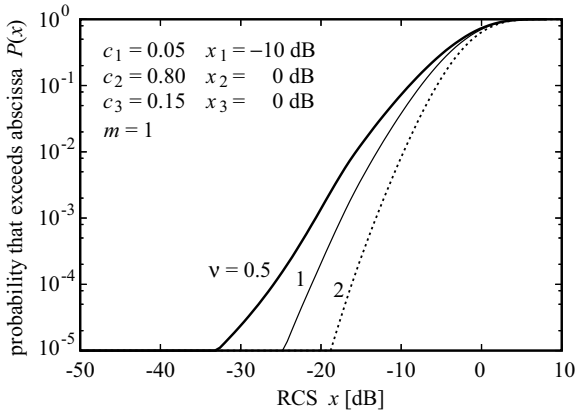

Fig. 7. Dependence of the probability on the shape parameter of the category 3 reflection object (single pulse detection).

radar resolution increases as a decrease of the pulse width, then radar echoes tend to be spiky in time or distance range domain. The conventional estimation was optimistic. Therefore, we proposed the method of suppressing clutter by using the reception power conversion. The conversion table smoothed the spikes in reception signal. The distribution and the conversion table depended on the existence probabilities and the shape parameter. It is important to know the accurate parameters by measurements.

REFERENCES

[1] M. I. Skolnik, *Introduction to Radar Systems*, , 3rd ed. New York: McGraw-Hill, 1980.

[2] E. Jakeman and P. N. Pusey, "A model for non-Rayleigh sea echo," *IEEE Trans. Antennas & Propagat.*, vol. AP-24, no. 6, pp. 806–814, Nov. 1976.

[3] R. J. Fogler, L. D. Hostetler, and D. R. Hush, "SAR clutter suppression using probability density skewness," *IEEE Trans. Aerospace & Electronic Syst.*, vol. 30, no. 2, pp. 622–626, Apr. 1994.

[4] D. M. Drumheller, "Estimating matched filter amplitude probability functions by failure rate analysis," *IEEE Trans. Aerospace & Electronic Syst.*, vol. 35, no. 2, pp. 627–635, Apr. 1999.

[5] Y. Chen, E. Gunawan, Y. Kim, K. S. Low, C. B. Soh, and L. L. Thi, "UWB microwave breast cancer detection: generalized models and performance prediction," in *Proc. IEEE EMBS Annual International Conference*, Aug./Sept. 2006, pp. 2630–2633.

[6] S. Vasudevan and J. L. Krolik, "Refractivity estimation from radar clutter by sequential importance sampling with a Markov model for microwave propagation," in *2001 IEEE International Conference on Acoustics, Speech, and Signal Processing (ICASSP '01)*, vol. 5, pp. 2905–2908, 2001.

[7] E. Jakeman and R. J. A. Tough, "Non-Gaussian models for the statistics of scattered waves," *Advances in Physics*, vol. 37, no. 5, pp. 471–529, 1988.

[8] A. Papoulis, *Probability, Random Variables, and Stochastic Processes*, , 3rd ed. Boston: WCB McGraw-Hill, 1991.

[9] R. Barakat, "First-order statistics of combined random sinusoidal waves with applications to laser speckle patterns," *Optica Acta*, vol. 21, no. 11, pp. 903–921, Nov. 1974.